The Extent and Rate of the Appearance of the Major 110 and 30 kDa Proteolytic Fragments during Post-Mortem Aging of Beef Depend on the Glycolysing Rate of the Muscle and Aging Time: An LC–MS/MS Approach to Decipher Their Proteome and Associated Pathways

Mohammed Gagaoua, Declan Troy, Anne Maria Mullen

HAL Id: hal-04156215
https://hal.inrae.fr/hal-04156215

1   **The extent and rate of the appearance of the major 110 and 30 kDa proteolytic fragments**

2   **during post-mortem aging of beef depend on the glycolysing rate of the muscle and aging**

3   **time: an LC-MS/MS approach to decipher their proteome and associated pathways**

4

5   Mohammed Gagaoua[1]*, Declan Troy[1], Anne Maria Mullen[1]

6

7   [1] Food Quality and Sensory Science Department, Teagasc Ashtown Food Research Centre,

8   Ashtown, Dublin 15, Ireland

9

10 ***Correspondence:** Dr. Mohammed Gagaoua

11 mohammed.gagaoua@teagasc.ie ; ORCID: 0000-0001-6913-3379

12

13 **Abstract**

14 Post-mortem (p-m) muscle undergoes a myriad of complex physical and biochemical changes,

15 prior to its conversion to meat, which are influential on proteolysis and hence tenderisation. A

16 more in-depth understanding of the mechanisms underpinning these dynamics is key to

17 consistently providing tender beef. Using an LC-MS/MS approach, with state-of-art mass

18 spectrometry Q Exactive HF-X, the proteome and associated pathways contributing to the

19 appearance of the proteolytic breakdown products appearing over 14 days p-m, at two important

20 molecular weights (110 and 30 kDa) on 1D SDS-PAGE gels, have been investigated in beef

21 *Longissimus thoracis et lumborum* muscles exhibiting four rates of pH decline differentiated on

22 the basis of time@pH6 (fast glycolysing < 3h; medium 3 -5 h; slow 5 − 8 h; and very slow 8+

23 h). Both 110 and 30 kDa bands appeared during aging and increased in intensity as a function of

24 p-m time in a pH decline-dependent manner. The 110 kDa band appeared as early as 3h p-m and

25 displayed an incremental increase in all groups through to 14 d p-m. From 2 d p-m, this increase

26 in abundance during aging was significantly ($P < 0.001$) influenced by glycolytic rate: fast > or

27 = medium > slow > very slow. The day 2 p-m appearance of the 30 kDa band was most evident

28 for fast glycolysing muscle with little or no evidence of appearance in slow and very slow. For

29 day 7 and 14 p-m the strength of appearance was dependant on glycolysing groups: fast >

30 medium > or = slow > very slow. LC-MS/MS analysis yielded a total of 22 unique proteins for

31 the 110 kDa fragment and 13 for the 30 kDa, with 4 common proteins related to both actin and

32 fibrinogen complex. The Gene Ontology analysis revealed a myriad of biological pathways are

33 influential with many related to proteins involved primarily in muscle contraction and structure.

34 Other pathways of interest include energy metabolism, apoptotic mitochondrial changes,

35 calcium and ion transport, etc. Interestingly, most of the proteins composing the fragments were

36 so far identified as biomarkers of beef tenderness and other quality traits.

37 **Keywords:** Beef tenderization; pH decline; Myofibrillar proteins; Metabolism; Proteomics

Introduction

Post-mortem (p-m) animal muscles undergo myriad and sophisticated physical and biochemical changes, which are responsible of their transformation into meat [1, 2]. These changes are first accompanied by a decrease in pH and temperature, described to be the former drivers of meat tenderization [3], hence affecting the osmotic pressure, the ionic strength of the muscle and the expressible juice[1, 2]. Furthermore, the extent of glycolysis and other energy metabolic pathways have a strong influence on many meat quality traits [4-6]. Their rate was considered to be a key determinant of tenderness through their impact on temperature and pH fall consequently orchestrating the activity of the endogenous muscle proteolytic enzymes [1, 7] and the apoptosis onset and development of *rigor mortis*[1, 8]. Many proteolytic systems such as calpains/calpastatin, cathepsins/cystatins, caspases/serpins, proteasomes and serine peptidases have been investigated *in vitro* for their impact on muscle degradation and beef tenderization [8-10]. Much of the research on p-m muscle protein changes has concentrated on the breakdown of the myofibrillar proteins with the main effects observed through fragmentation of proteins along the z-disc of the sarcomere [2, 11-13]. Therefore, a weakening and denaturation of muscle proteins and myofibrillar structure occur as a result of p-m storage of carcasses or meat cuts, which in turn leads to the tenderness experienced in cooked meat.

Recently and through the use of proteomics, muscle protein degradation has been further evidenced to be linked to energy metabolism (appearance of fragments of both glycolytic and oxidative enzymes including molecules from mitochondria), programmed cell death, heat shock proteins and oxidative stress among others [13-16]. However, inconsistencies in protein degradation occur and they are not fully understood. Among the studies that approached this aspect, some of them suggested that the underlying mechanisms are linked to the initial pH and extent of pH decline during the process of p-m glycolysis[17]. Others appointed the differences in the contractile and metabolic properties to variations in muscle fibres and their plasticity[6]. Recently,

63   and thanks to the use of liquid chromatography (LC) coupled to mass spectrometry (MS),

64   Farouk's group from New Zealand highlighted that beef tenderization is likely to be

65   compartmentalised by ultimate pH[18] when muscles were categorised as having low ($\leq$ 5.79),

66   medium (5.80 − 6.19) and high ($\geq$ 6.2) ultimate pH. Further, the same group identified that

67   depending on the ultimate pH category, different protein patterns and degradation rates of

68   structural proteins can be observed [19]. However, the threshold level used of ultimate pH above

69   5.8 is considered by most beef companies, especially in Europe, to be of lower and more

70   variable eating quality, hence leading to dark-cutting meat [20, 21]. Accordingly, in this study we

71   targeted only carcasses that reached a pH of 5.8 or less in the loin muscle at the end of the

72   maturation period (48 h p-m) and we considered for the first time four pH decline categories

73   based on the time@pH6: fast < 3 h; medium 3 − 5 h; slow 5 − 8 h and very slow 8+ h. Hence,

74   we hypothesized that the proteolysis extent will depend on the glycolysing rate of the p-m

75   muscle. The identification of the proteome affected by the biochemical processes occurring

76   during meat aging would contribute to deeper our understanding of the phenomenon of p-m beef

77   aging. Therefore, this study aimed to decipher by means of LC-MS/MS and using the latest MS

78   instrument in the benchtop Orbitrap series, the Q Exactive HF-X, the proteomic pathways

79   involved in the appearance of two major proteolytic fragments running at two different

80   molecular weights (low and high), whose intensities increased by increasing the aging time.

81   **Materials and Methods**

82   *Animals, slaughtering and muscle sampling*

83   Seventy eight crossbred beef cattle, representative of a typical commercial population, were

84   slaughtered at an industrial meat plant (Dawn Meats group, Ballyhaunis, Republic of Ireland).

85   From these, 12 heifers and 12 steers were selected to fit four pH decline rates as described

86   below (n=3 per decline group for each gender). The animals were of similar age at slaughter (24

87    $\pm$ 1.9 months old) and carcass weight (325 $\pm$ 47 kg), and all finished to a specified fat cover

88   score (9.6 ± 1.4) and conformation (6.8 ± 2.1), both on a EUROP 1 – 15 scale. Slaughtering was

89   performed in the morning under standardised conditions. Briefly, all animals were captive bolt

90   stunned followed by exsanguination from the jugular vein and stun time was recorded as the

91   point of reference for pH measurements. Then, the carcasses were dressed following the

92   conventional commercial practices in compliance with the EU regulations (Council Regulation

93   (EC) No. 1099/2009). Between 30 – 40 min post exsanguination, carcasses were split into two

94   sides and then chilled at 10°C for 11 – 12 h, followed by storage in a 0°C chill until 48 h p-m.

95   Samples of *Longissimus thoracis et lumborum* (LTL, mixed fast oxido-glycolytic) muscles were

96   collected at four different p-m times (day 0 being 3h p-m, day 2 (48 h), day 7 and day 14). LTL

97   muscle samples were removed, taking care to avoid connective tissue and subcutaneous or inter-

98   muscular fat at 3hr p-m near the 4th lumbar from the right hand side of each carcass and

99   immediately frozen in dry ice and transported to Teagasc, Ashtown for storage at -80°C.

100   Second, striploin meat samples from the same carcasses side were taken on day 2 when they

101   were quartered at the 5th rib. For this purpose, one steak of 2.5 cm thick close to the pH

102   measurement point was cut into three parts (left, middle and right). The middle part was

103   immediately used to take very carefully biopsies (day 2) free of fat and connective tissue. The

104   two other parts were vacuum packaged and aged at 4°C for 7 (left) and 14 days (right) to sample

105   the remaining biopsies. Storage of all the samples was performed at −80 °C until biochemical

106   analyses.

107   *pH measurement, modelling and kinetic data analysis*

108   The pH of the LTL muscle was monitored by means of a portable pH meter (Orion Research

109   Inc., Boston, USA) initially adjusted for muscle temperature and calibrated by two pH buffers

110   being 4.0 and 7.0 before each set of measurements. pH was recorded at the 4th lumbar location at

111   a depth of 4 cm at hourly intervals up to 8 h p-m and another measurement at 48 h p-m

112   considered as the ultimate pH. From the experimental curves of pH decline p-m of each animal,

113   an exponential equation with time p-m was used for fitting of the pH profile for rate constant

114   determination as a function of time using the parameterisation of an exponential decay

115   function[22]:

$$K = a - b \, x \, e^{(-c \, x \, t)}$$

117   where K represents the parameter,

118   a, its ultimate value,

119   b, the extent of its decline,

120   c, the rate of its decline,

121   and t, the time (h) p-m.

122   The variables a, b and c were calculated by minimizing the sum of squared residuals based on

123   the non-linear method of Newton Raphson algorithm [23]. The rate of pH decline was considered

124   in this study to characterize the animals in addition to the time @ pH 6.0 that allowed defining

125   four pH decline categories: fast < 3 h; medium 3 – 5 h; slow 5 – 8 h and very slow 8+ h.

126   ***Protein extractions and quantification***

127   Portions of the frozen muscle tissue samples from the four sampling times were used for

128   muscle proteins extractions. Briefly, 500 mg pieces of muscle were cut and weighed at – 20°C

129   to reduce artifactual protein degradation, subsequently incubated at 4°C for 10 min in 10 mL of

130   freshly prepared extraction buffer using Milli-Q purified water and containing 8 M urea, 2 M

131   thiourea, 1% DL-Dithiothreitol, 2% CHAPS, and 1.8% Pharmalyte® 3 - 10 (GE Healthcare,

132   Uppsala, Sweden). Next, the meat sample was homogenized for 40 sec (2 × 20 s with 20 s break

133   between bursts) using a T25 digital Ultra-Turrax® (IKA, Germany) at a high speed (15,000

134   rpm). The homogenates were incubated with shaking for 30 min on wet-ice, followed by a 30

135   min centrifugation at 10000 × g (Eppendorf 5424R, Eppendorf AG, Hamburg, Germany) and at

136   4°C to remove fat, insoluble proteins and any non-extracted cellular components. The pellet was

137   then solubilised in 5 mL of the same buffer and centrifuged under the same conditions for 10

138   min at 4°C. The supernatant was collected, fractionated and transferred into Eppendorf tubes

139   and stored at -80°C prior the proteomic analysis. Protein concentrations in triplicate were

140   determined using the Bio-Rad Protein Assay Kit (Bio-Rad Laboratories, Hercules, CA, USA)

141 based on the Bradford method. Bovine serum albumin (BSA) at a concentration of 1 mg/mL

142 was used as standard. The extraction yield was the same within each sampling time for the four

143 pH decline categories.

144 ***1D SDS-PAGE electrophoresis***

145 Post-mortem proteolytic patterns were examined in 96 muscle protein extracts representing

146 four sampling times (day 0, 2, 7 and 14) across the four pH decline categories (fast (F), medium

147 (M), slow (S) and very slow (VS)) using one dimensional (1D) Sodium dodecyl sulphate –

148 polyacrylamide gel electrophoresis (SDS-PAGE). This was carried out according to Laemmli [24]

149 using 12% resolving and 4% stacking gels. Briefly, the protein extracts were first mixed at a

150 ratio of 1.0:1.0 with sample buffer Laemmli 2× concentrate (#S3401, Sigma-Aldrich, St. Louis,

151 USA) containing 4% w/v SDS, 20% v/v glycerol, 10% v/v β-mercaptoethanol, 125 mM Tris

152 (pH 6.8) and 0.004% bromophenol blue, incubated at room temperature for 10 min and then

153 heated (75°C) for 15 min in a standard block heater (VWR International). The denatured protein

154 extracts in duplicate (20 μg per lane, 192 lanes in total) were then loaded and subjected to

155 separate on a Mini-PROTEAN Tetra Cell system (Bio-Rad Laboratories, Hercules, CA, USA)

156 for 3 h at 120 v using a TGS running buffer (#T7777, Sigma-Aldrich, Saint Louis, MO 63103,

157 USA), which contains 25 mM Tris (pH 8.6), 192 mM glycine and 0.1% SDS. For each gel and

158 in the first lane, 5 μL of a broad-range standard molecular weight marker (10–250 kDa,

159 Precision Plus Protein™ Dual Color Standards, #161-0374, Bio-Rad Laboratories, Segrate-

160 Milano, Italy) was included as a standard. Following completion of the separation, the gels were

161 first washed twice in Milli-Q water for 5 min each time and stained overnight in 20 mL

162 Coomassie Brilliant Blue G-250 based protein stain solution (EZBlue® gel staining reagent,

163 Sigma-Aldrich, St. Louis, USA) with gentle shaking. The following morning, the gels were de-

164 stained under shaking with Milli-Q water for 4h and washed twice before acquisition in

165 transmission-scan mode by calibrated transparency densitometric scanner (GS-800, Bio-Rad)

166   using Bio-Rad Quantity One-4.5.2 software. Background subtraction was performed using the

167   "lane background" function.

168   For band intensity quantification, all the protein bands in the scanned image gels (700 dpi and

169   16-bit) were quantified by Un-Scan-It gel 6.5 analysis program (Silk Scientific, Orem, UT) to

170   estimate the molecular weights and optical intensities of the bands. The quantification of the

171   band intensities aimed to identify the significant differences across pH decline group category

172   and aging time. The data were exported to a Microsoft Excel spreadsheet and the densitometry

173   of each band was normalized to the total density of the corresponding molecular weight in the

174   entire row and expressed in arbitrary units (AU). Further, the data matrix was normalized per pH

175   decline group and aging time. Then, a one-way ANOVA was used to detect the significant

176   protein bands appearing as a consequence of proteolysis and differing with aging time across the

177   four pH decline categories. Accordingly, two major and different proteolytic fragments were

178   identified, these being the 30 and 110 kDa (**Figure 1**), which were considered of interest for LC-

179   MS/MS identification and bioinformatics analyses.

180   *LC–MS/MS analysis*

181   The two proteolytic fragment bands appearing with an increase intensity during aging (at Day

182   2, 7 and 14) were excised by hand using sterile and disposable scalpels, de-stained, and prepared

183   by reduction/alkylation, digestion by trypsin (Promega), peptide extraction, and drying [25] prior

184   to LC-MS/MS using a Q Exactive HF-X hybrid quadrupole-Orbitrap mass spectrometer

185   (Thermo Fisher Scientific). The hydrolysis of the bands was carried out with 48 μL of a 25mM

186   ammonium bicarbonate buffer –12.5 ng/μL trypsin solution (Promega) per band for 5 h in an

187   oven at 37 °C. A volume of 30 μL buffer was added periodically during hydrolysis so that the

188   bands were always covered with liquid. The extraction of the peptides was carried out under

189   ultrasonication for 15 min with 38.4 μl of 99.95% acetonitrile – 0.05 % trifluoroacetic acid.

190   Then, the supernatant was transferred into 500 μL Eppendorf tubes and dry concentrated using a

191 Speedvac for 2 h. The volume was adjusted exactly to 20 μL with a solution of isotopologic

192 peptides (50 pmol/μL) that is diluted 18 times in a 0.05 % TFA solution (internal quality

193 control). After passing through the ultrasonic bath (10 min), the entire supernatant was

194 transferred to an HPLC vial prior to LC-MS/MS analysis.

195 The separation step was carried out using a nano-HPLC Ultimate 3000 whereby, 2 μL of the

196 protein hydolysate were first injected after pre-concentrated and desalted at a flow rate of 30

197 μL/min on a C18 pre-column 5 cm length × 100 μm (Acclaim PepMap 100 C18, 5μm, 100A

198 nanoViper) equilibrated with Trifluoroacetic acid 0.05% in water to remove contaminants that

199 could potentially disrupt the efficiency of the mass spectrometry analysis. After 6 min, the

200 concentration column was switched online with a nanodebit analytical C18 column (Acclaim

201 PepMap 100 - 75 μm inner diameter × 25 cm length; C18 - 3 μm -100Å - SN 10711310)

202 operating at 400 nL/min equilibrated with 96 % solvent A (99.9 % H_2O, 0.1 % formic acid). The

203 peptides were then separated according to their hydrophobicity, thanks to a gradient of solvent

204 B, a solution of acetonitrile (ACN / FA-99.9 / 0.1) of 4 to 25% in 50 minutes. The nanoHPLC is

205 coupled via a nanoESI source to an Orbitrap Q Exactive HFX mass spectrometer that operates in

206 data dependent mode. The parent ion is selected in the orbitrap cell (FTMS) at a resolution of

207 60,000. Each MS analysis is succeeded by 18 MS/MS with analysis of the spectra fragments at a

208 resolution of 15,000, microscan range of m/z 375 − 1600 and 60 s exclusion duration. The

209 MS/MS spectra were analyzed using Proteome Discoverer V1.4.1 (ThermoFisher) and

210 compared to *Bos taurus* Uniprot database (37,513 sequences, reference UP000009136_2020)

211 using Mascot V 2.5 (http://www.matrixscience.com) with request parameters set: precursor

212 mass tolerance to 10 ppm and fragment mass tolerance to 0.02 Da. For variable modifications, a

213 maximum of two missed cleavages sites of trypsin was allowed including carbamidomethylation

214 (C), methionine oxidation (M) and deamidation (NQ). Protein identification was validated when

215 at least 2 unique peptides originating from one unique protein accession number showed

216 statistically significant identity above Mascot scores of ≥ 28 with a False Discovery Rate (FDR)

217   of 1%. Furthermore, for the purpose of this study, we increased the confidence to a minimum of

218   4 unique peptides to accurately validate the proteins composing the 30 and 110 kDa proteolytic

219   fragments.

Bioinformatics analyses

221   The LC-MS/MS yielded a total of 22 unique proteins for the 110 kDa fragment and 13

222   proteins for the 30 kDa (**Table 1** and **Table 2**), with 4 common proteins. The bovine UniprotIDs

223   of the 31 proteins were converted[13] into the human orthologs EntrezGeneID to take advantage of

224   the most complete annotation available. Therefore, both bovine and human UniprotIDs were

225   indexed in the database and used. The process enrichment clustering was performed on

226   Metascape® (https://metascape.org/) based on Kyoto Encyclopedia of Genes and Genomes

227   (KEGG) pathways, Gene Ontology (GO) Biological Processes, and Reactome gene sets on the

228   whole proteins as one dataset and for each proteolytic band fragment as separate datasets.

229   Metascape® uses the hypergeometric test and Benjamini–Hochberg p-value correction algorithm

230   to display the first statistically significant enriched ontology terms. In this study, the terms with

231   a P-value < 0.05, a minimum count of 3, and an enrichment factor >1.5 (ratio between the

232   observed counts and the counts expected by chance) were considered. Representative terms with

233   a similarity score > 0.3 were clustered together based on their membership similarities and

234   visualized in a network.

235   From the protein-protein interaction (PPI) network generated by Metascape®, the molecular

236   complex detection (MCODE) algorithm was then used to detect densely connected regions (with

237   default parameters) in the protein interaction network (neighbourhoods) if there are more than

238   two proteins in a network. Pathway and process enrichment analysis were performed to each

239   MCODE component independently and the significant scoring terms by p-value (Benjamini–

240   Hochberg corrected) were retained as the functional description of the corresponding

241   components. A unique colour was assigned to every MCODE network. A second PPI network

242   linking the 31 proteins from the 110 and 30 kDa polypeptides, including the molecular function

243   was generated from the web-based search STRING database (https://string-db.org/). As an

244   additional process, Metascape® was utilized to exhibit distribution of the 31 proteins among the

245   two proteolytic fragments, based on a Circos plot which displays overlap and functional

246   connections between the proteins. Subsequently, the known and potential targets based on the

247   enriched terms among the two proteolytic fragments generated by the pathway and process

248   enrichment analyses were compared and displayed by means of hierarchical heatmap clustering

249   emphasizing the significant clusters.

250   Potential quantitative trait loci (QTL) were assessed using the ProteQTL tool included in

251   ProteINSIDE (http://www.proteinside.org/) among the 31 proteins of the two proteolytic

252   fragments appearing during aging. ProteQTL interrogates a public library of published QTL in

253   Animal QTL Database (https://www.animalgenome.org/QTLdb) that contains cattle QTL and

254   association data curated from published scientific articles. In this study, we considered three

255   beef quality attributes available that are tenderness score, shear force and meat color lightness

256   (L^*). Finally, a computational prediction of the putatively secreted proteins was performed on

257   ProteINSIDE tool (http://www.proteinside.org/) identifying those potentially secreted through a

258   signal peptide using the Signal P algorithm or by unconventional pathways of secretion (not

259   involving a signal peptide) using the Target P algorithm.

260   ***Statistical analyses***

261   The densitometry data of the protein fragments were analysed using the General Linear

262   Model procedure of the SAS statistical software (SAS 9.3, SAS Institute INC, Cary, NC, USA).

263   The test effects were pH decline group (fast, medium, slow and very slow) as the whole plot and

264   aging time as the subplot (day 0, 2, 7 and 14). Gender effect was further considered included as

265   random effect and no significant effect was observed and consequently removed. Least squares

266   means were separated using Tukey test and considered significant if p-value is < 0.05. All

267   quantitative data were expressed as mean ± standard deviation (SD). A principal component

268   analysis (PCA) of pH decline values was carried out using XLSTAT 2018.2 (AddinSoft, Paris,

269   France) to highlight the separation of the pH decline groups.

270   **Results**

271   *pH decline and protein changes over aging p-m time*

272   **Figure 1a** shows the expected, clear separation of the four pH decline categories on the first

273   two principal components. Individual variation is slightly higher for the fast glycolysing group

274   (for which no overlap was observed with the other categories), compared to the other groups

275   which are mostly grouped together, especially for the very slow glycolysing carcasses projected

276   on the right. The divergence in the p-m pH decline curves among the four glycolysing groups

277   was further confirmed by the significant differences ($P < 0.001$) in the pH decline rates (k

278   values) computed for each glycolysing category (**Figure 1b**): 0.56 ± 0.08 pH unit/h for fast, 0.32

279   ± 0.04 pH unit/h for medium, 0.22 ± 0.02 pH unit/h for slow and 0.13 ± 0.03 pH unit/h for very

280   slow group. **Figure 1c** shows a representative SDS-PAGE protein profile of the M. *longissimus*

281   *thoracis et lumborum* muscle extracts at four different aging times sampled early p-m at day 0

282   (3h) and during aging at 2, 7 and 14 days p-m. The densitometry analysis on each gel (192 lanes

283   in total) revealed the appearance of two major proteolytic fragment bands during p-m beef

284   aging: 110 kDa (**Figure 1d**) and 30 kDa (**Figure 1e**). The relative abundance of the two protein

285   fragments differ significantly ($P < 0.001$) within pH decline categories and across aging times

286   with significant abundances by increasing the aging time period (**Table S1** and **Table S2**).

287   At day 0, only the 110 kDa fragment was appearing whatever the pH decline (in few animals

288   only) with the highest abundance in medium glycolysing group and lowest in the very slow

289   group (**Figure 1d**). At days 2 and 7 p-m, the abundance of this fragment was significantly ($P <$

290   0.001) higher for the fast and medium glycolysing rate carcasses compared to the slow and very

291   slow (**Table S1**). At 14 days p-m a significant separation of the four curves is evident with

292   greater abundance for the fast group followed respectively by the medium, slow and very slow

293   glycolysing categories. A stepwise increase in abundance from day 0 to day 14 was evident for

294   all four pH decline categories. For the 30 kDa protein fragment, it first appeared at day 2 p-m

295   (**Table S2**). Levels increased incrementally in all four groups from day 2 to day 14 p-m with the

296   highest levels consistently observed in the fast glycolysing). At 2 days p-m, this fragment was

297   mostly absent for the slow glycolysis (present in one carcass only) and not visible yet for any of

298   the very slow carcasses (**Table S2**). The fragment was detectable in all the carcasses at 7 and 14

299   days p-m and as with the 110 kDa, greater abundances of the 30 kDa protein fragments were

300   observed at both days for the fast glycolysing carcasses followed respectively by the medium,

301   slow and very slow glycolysing categories (**Figure 1e**). The modelling of the relative

302   abundances of the two protein fragments (**Figure 1f,g**) confirmed the trend of appearance

303   described above, *i.e,* fastest for the fast glycolysing category, slower in medium and slow

304   categories and slowest in the very slow glycolysing muscles, with significant separation of the

305   curves within aging time and across the glycolysing rates. Further, the regression of the

306   modelled protein bands abundances of the two fragments at 14 days p-m revealed that their

307   appearance is concomitant with meat aging, especially for the fast group for which a high r-

308   square > 0.98 was observed (**Figure 1h**). Finally, the findings of this trial indicated a greater

309   degree of proteolysis in the fast glycolysing muscles in line with the earlier appearance of the

310   110 and 30 bands and the higher levels at day 14 p-m, which are indicative of more rapid

311   proteolytic activity.

312   ***LC–MS/MS identification of the proteins composing the two major proteolytic fragments***

313   To decipher the proteome content of the proteolytic fragments appearing at the 110 and 30

314   kDa zones during beef aging and the associated pathways, an LC-MS/MS approach provided

315   identification of 22 unique proteins (with a minimum of 4 unique peptides) for the 110 kDa

316   fragment (**Table 1**) and 13 proteins for the 30 kDa (**Table 2**). Four proteins, namely, ACTA1

317   (α-actin) and FGA, FGB and FGG (Fibrinogen α, β and γ chains, respectively) were common to

318   the two proteolytic fragments (**Figure 2a**).

319   The 22 proteins of the 110 kDa proteolytic fragment belong to five main biological pathways

320   (**Table 1**) from which half (n = 11) were (i) muscle contraction and structure proteins including

321   three myosin heavy chains isoforms (MYH1, MYH2 and MYH7), ACTA1, actinins (ACTN2

322   and ACTN3), nebulin (NEB), plectin (PLEC) and binding proteins (MYBPC1, MYBPC2 and

323   MYOM2). The (ii) catalytic and energy metabolism pathway grouped four enzymes: PYGM,

324   OGDH, PHKB and NNT (**Table 1**). These were followed by three (iii) fibrinogen complex

325   proteins FGA, FGB and FGG and (iv) proteolysis with two proteins: F2 which is a prothrombin

326   and PSMD1 which is a subunit of the 26S proteasome. The last pathway grouped two other

327   proteins (v) involved in calcium-binding and apoptotic mitochondrial changes, these being

328   ATP2A1 and SRL (**Table 1**). Thirteen of the 22 proteins are secreted proteins, from which 5 are

329   through a signal peptide (FGA, FGB, FGG, F2 and SRL) and 8 through pathways that do not

330   involve a signal peptide (ACTA1, ACTN2, ACTN3, NEB, PLEC, PYGM, PSMD1 and

331   ATP2A1).

332   The 13 proteins of the 30 kDa proteolytic fragment belong to four main biological pathways

333   (**Table 2**) with three pathways common to the 110 fragment. Three proteins were from the (i)

334   muscle contraction and structure, these being ACTA1, fast Troponin T (TNNT1) and MYL1

335   that is a myosin light chain. From (ii) the catalytic and energy metabolism pathway two

336   enzymes   were   identified: creatine   kinase   M-type   (CKM)   and   mitochondrial   2-

337   oxoglutarate/malate carrier protein (SLC25A11). The third pathway grouped the three (iii)

338   fibrinogen complex proteins FGA, FGB and FGG (**Table 2**) followed by the last pathways,

339   which grouped five protein-binding, calcium and ion transport entities: B2M (beta-2-

340   microglobulin), VDAC3 (voltage-dependent anion-selective channel protein 3), PHB

341   (prohibitin), CA3 (carbonic anhydrase 3) and APOBEC2 (C->U-editing enzyme APOBEC-2).

342   Seven of the proteins of this fragment are secreted proteins from which four are through a signal

343   peptide (FGA, FGB, FGG and B2M) and 3 through pathways that do not involve a signal

344   peptide (ACTA1, VDAC3 and PHB).

345   ***Bioinformatics: functional enrichment analysis, clustering and protein-protein interaction***

346   The process enrichment and cluster analysis pathways on the identified proteins based on GO

347   and KEGG allowed the identification of 5 top and significant enriched terms (functional

348   clusters) across the protein lists for the 110 kDa fragment (**Figure 2b**) and 3 for the 30 kDa

349   (**Figure 2c**). The enrichment of the combined 31 proteins (two lists) highlighted in the order of

350   importance (i) muscle filament sliding, (ii) fibrinogen complex and (iii) striated muscle

351   contraction pathways as the top 3 enriched terms (**Figure 3d**). The heatmap comparing the

352   protein lists and pathways between the two proteolytic fragments summarized the top 8 enriched

353   term clusters (**Figure 3e**). The graph revealed that both muscle filament sliding (GO:0030049)

354   and fibrinogen complex (CORUM:6417) are common to the two polypeptides (statistics details

355   are given in **Table 3**), whereas anion transport term (GO:0006820) was specific to the 30 kDa

356   fragment only and the terms skeletal muscle adaptation (GO:0043501), striated muscle

357   contraction (GO:0006941), cell-substrate junction assembly (GO:0007044), energy derivation

358   by oxidation of organic compounds (GO:0015980) and positive regulation of cation

359   transmembrane transport (GO:1904064) were specific to the 110 kDa fragment (**Table 3** and

360   **Figure 2e**). The association of these enriched terms and their functional enrichment was

361   visualized by the network of **Figure 2f** showing once again the importance of muscle filament

362   sliding and fibrinogen complex biological processes on beef aging. Furthermore, three

363   significant sub-networks of high local network connectivity (MCODE 1–3) with 15 hub genes

364   (proteins) were revealed from the PPI network based on MCODE analysis (**Figure 2g,h**). Of

365   these, MCODE_1 evidencing the striated muscle contraction/filament sliding (ACTN2, ACTN3,

366   MYBPC1, MYBPC2, NEB (110 kDa fragment), MYL1 and TNNT3 (30 kDa fragment)) had the

367　highest MCODE score (**Figure 2g**). MCODE_2 grouped FGA, FGB, FGG (for the two

368　proteolytic fragments we targeted) and F2 (for 110 kDa fragment only) belonging to the

369　fibrinogen complex and fibrinolysis pathway. MCODE_3 with the lowest MCODE score

370　grouped 4 proteins that are OGDH, PYGM, PSMD1 (for 110 kDa fragment only) and VDAC3

371　(specific for the 30 kDa fragment) for the energy metabolism, anion transport and regulation

372　pathway. The interconnectedness of these pathways was evidenced by the STRING network

373　highlighting two major sub-networks (**Figure 3**), the striated muscle contraction/filament sliding

374　(n = 12 proteins) and the fibrinogen complex and fibrinolysis (n = 4 proteins), that were both

375　linked through the major components of the Z-line, alpha-actinin-2 (ACTN2).

376　**Discussion**

377　　Tenderness is considered by consumers as a very important palatability trait driving the

378　overall liking of cooked beef or influencing (re)purchasing decisions. However, inconsistency in

379　the final eating quality has been identified as one of the major challenges facing the beef

380　industry due to the wide range of factors impacting beef tenderness [26]. Among the post-slaughter

381　and intrinsic factors, we hypothesised that variation in beef tenderness is related to differential

382　response at the molecular/biochemical level within muscles during the early p-m carcass

383　handling and aging periods. This trial has clearly demonstrated that during these periods and

384　regardless of the pH decline rate, a myriad of biological pathways are being altered and these

385　pathways relate to muscle contraction and structure, energy metabolism, apoptotic

386　mitochondrial changes, calcium and ion transport, etc. In addition, we have demonstrated that

387　these changes contribute to the appearance of two protein bands, which are newly created during

388　the p-m period. While knowledge on these bands have increased over the past decades [2, 11, 17, 27,

389　28], this study is the first to decipher the proteome and associated pathways which are connected

390　with the appearance of the 110 and 30 kDa bands. Further, this study confirmed previous

391   suggestions [7] that the rates of the appearance of these protein band fragments depend on the

392   glycolysing rate of the muscle (pH decline category) as well as aging time.

393   Although since it was first proposed as a band of interest by Young, et al. [29], the 110 kDa has

394   only been the focus of a handful of papers. Its importance was confirmed in the following

395   decades [27] with the preliminary sequencing of this fragment taking place at the end of 90's by

396   Troy, et al. [30]. The authors demonstrated an 80% homology with human C-protein for the first

397   17 amino acids sequenced. Our study has confirmed the presence of the C-protein, which is in

398   fact the myosin-binding protein C represented in this study by two isoforms (MYBPC1, slow-

399   type and MYBPC2, fast-type) in addition to 20 other proteins (**Table 1**). On the other hand, the

400   30 kDa band has been more extensively studied and was identified as an important marker of

401   tenderization and a useful index to the progress of aging and proteolysis extent of muscle

402   proteins degradation [2, 27, 28, 31-33]. The identity of this fragment was ascribed to originate from

403   troponin T degradation [34, 35], but also proposed to contain actin fragments[1]. The LC-MS/MS

404   used in this study enabled the identification of both troponin T (TNNT3) and actin (ACTA1) in

405   keeping with the literature [1, 12, 16, 36]. However, we have also provided evidence that fragments

406   from 11 other proteins are identifiable in this band (**Table 2**). Taken the above together, this

407   study revealed using an appropriate *a priori* method (LC-MS/MS approach) that more than one

408   protein composes the two protein proteolytic bands. These novel insights about such

409   fragmentation products whose appearance are enhanced with aging and whose biological

410   pathways are very important (for reviews: [1, 5, 13]), are potentially useful in more thoroughly

411   understanding the processing underpinning beef tenderization. Interestingly, most of the proteins

412   represented in these protein bands, as summarized in **Table 1** and **Table 2,** have also recently

413   been identified in large integromics and proteomics studies[4, 13] to be biomarkers of beef

414   tenderness (17 of 22 for the 110 kDa fragment and 9/13 for the 30 kDa) and colour traits (14/22

415   for the 110 kDa and 8/13 for the 30 kDa). Further, some of the proteins were reported to

416   correlate with pH values and certain are drivers of pH decline (**Table 1** and **Table 2**). In the

417   following, we briefly present and discuss the main biological pathways which are represented in

418   these two proteolytic protein bands appearing during p-m aging of beef *Longissimus thoracis*

419   muscle.

420   ***Key role of the striated muscle contraction/filament sliding pathway during the p-m beef***

421   ***aging period***

422   Almost half of the proteins (13 from 31) represented in both protein bands, but particularly

423   the 110 kDa band, emanate from the muscle structure and contraction pathway. The

424   predominance of this pathway adds further weight to the body of evidence linking the degree of

425   the alteration and weakening of myofibrillar and cytoskeletal proteins during aging to the extent

426   of proteolysis and meat tenderness development [5, 11, 13, 36, 37]. In fact, three interrelated GO terms

427   grouped these proteins originating from the different parts of the sarcomere (**Table 3** and **Figure**

428   **2f**), with most of them also reported in a recent beef tenderness integromics meta-analysis [13].

429   Identification of proteins from the different parts of the sarcomere suggests that muscle

430   structural breakdown occurs on the whole sarcomeric regions. Some of the identified proteins or

431   their products can have MWs lower than the 110 kDa band. These are likely to be migrating in a

432   cross-linked or aggregated form, a phenomenon that is reported previously [37]. Protein oxidation

433   might further influence the protein solubility and the formation of aggregates. One other reason

434   may be attributed to the existence of molecular complexes as proteins by their nature interact to

435   form stoichiometrically stable complexes. This was confirmed here by the identification of a

436   densely connected region of proteins (MCODE_1) from the striated muscle contraction/filament

437   sliding pathway, which interacts with a second one (MCODE_2) via alpha-actinin-2 (ACTN2)

438   (**Figure 3**) grouping the fibrinogen complex and fibrinolysis pathway (**Figure 2g,h**).

439   The action of endogenous muscle proteases on the myofibril structure can be postulated to be

440   at the origin of the appearance of many of these new protein bands [8, 9, 12, 36]. Among the

441   proteolytic systems, μ-calpain is the most investigated and known to be influenced by pH

442   decline [38], a fact which may have contributed to the more rapid p-m appearance of proteolysis

443   especially for the fast glycolysing carcasses in this study (**Figure 1f,g**). Indeed, a faster

444   glycolysis was reported to result in an early appearance of the autolyzed form of μ-calpain [38].

445   Caspases, the critical drivers of apoptosis, were also postulated to produce fragments early p-m

446   [39, 40] with MW of some proteins such as actin (ACTA1, identified in both bands in this study)

447   ranging from 14 to 32 kDa [1]. The role of cytoskeleton in apoptosis is well known and ACTA1 is

448   considered as a hallmark for apoptosis [1]. In addition, actin has been described as the first protein

449   targeted by executor caspases [1, 8], leading to a progressive upward trend of the appearance of the

450   major 30-32 kDa fragment, along with other lower MW fragments in p-m tissue[16, 36].

451   Proteasomes are further thought to play a role early p-m and some *in vitro* studies reported

452   activity in beef muscles up to one day [41] or 3 days [42]. On another hand, cathepsins B and L

453   activities during pre-rigor correlate positively with beef tenderness, especially in the fast

454   glycolysing muscles [7]. In agreement to our findings, an earlier study reported the appearance of

455   a band at 115 kDa from myosin heavy chain degradation following incubation of the muscle

456   with cathepsin L [43] which is like to equate to our 110 kDa band.

457   Identification of myosin superfamily members (MYH1, MYH2 and MYH7) in the 110 kDa

458   band agrees with the findings of Wu et al.[37] who focused on large proteins of beef muscle with

459   MW >100 kDa. Degradation of myosins, which are located in the thick filaments, and the

460   formation of new fragments at different MW have been demonstrated early p-m and during

461   aging [19, 36], exhibiting an important role in beef tenderness determination [13] as well as other

462   quality traits [4]. For example, myosin interacts with actin through the actin-myosin complex and

463   the myosin light chains, and if myosin, or the acto-myosin bond, is weakened during aging, the

464   tenderness of meat is affected [11, 12]. The identification of MYL1 (Myosin light chain 1/3) in the

465   30 kDa band is in line with the importance of this protein as a beef tenderness biomarker [13].

466   Myosin light chains are located near the heads of the myosins and the breakdown of the latter

467   may be at the origin of the appearance of the former.

468   The M-band and the Z-disk play also pivotal role in the assembly of the acto-myosin filament

469   systems. Two proteins which are located in the M-band have been identified in this study:

470   myomesin-2 (MYOM2) known also as M-protein [44] and CKM, the muscle isoform of creatine

471   kinase that binds to central domains of both myomesin and M-protein [45]. During p-m aging,

472   CKM is progressively fragmented [15, 16]. The rate of its fragmentation is associated with the rate

473   of energy depletion and pH decline, explaining its identification in this trial and in large

474   integromics studies as a robust biomarker of beef tenderness [13] and colour [4] and also as a QTL

475   of colour lightness (**Table 4**).

476   Identification of MYOM2 in the 110 kDa band could be partly explained by their strong

477   binding properties to myosins (**Figure 3**), which is in agreement with Wu et al.[37]. MYOM2 is a

478   member of the immunoglobulin superfamily composed of immunoglobulin-like and fibronectin

479   type III domains [44]. Several thick filament-associated proteins, also called myosin-binding

480   proteins, belong to this immunoglobulin superfamily, such as myosin-binding protein C

481   (MYBPC) anchored to the thick filament. MYBPC is a crucial component of the sarcomere and

482   an important regulator of muscle function. For example, as well as binding myosin and actin [46] it

483   also interacts with the giant actin-binding protein nebulin, identified in the 110 kDa band.

484   Worthy to note that nebulin is highly prone to proteolysis by endogenous muscle proteases such

485   as cathepsin L [9]. Since nebulin helps to link/anchor the thin filament firmly to the Z-disc,

486   weakening of this link can trigger subsequent alterations in the myofibril during aging [47]. In this

487   study, both isoforms of MYBPC formed a strong protein complex (MCODE_1) in the PPI

488   network (**Figure 2g,h**). MYBPC1 was also a QTL of beef shear force (**Table 4**). Therefore we

489   can postulate that MYBPC is of relevance when considering p-m aging of meat and in particular

490   that it is influential in the rate of appearance of the 110 kDa fragment, and possibly that of the

491   30 kDa band, depending on the rate of pH decline (**Figure 1h**). As MYBPC might play a

492   modulatory role in the regulation of actin-myosin interaction and by binding to both proteins it

493   may directly affect calcium sensitivity. In fact, the earlier studies that searched the impact of

494 calcium and proteases inhibitors on myofibrils have shown that MYBPC can be solubilized by

495 calcium ions [48]. The solubilisation of this protein due to the influx of calcium into the muscle

496 cells may be then partly responsible of the weakening of the myofibrils and possibly increase

497 their susceptibility to proteolytic degradation. In support of this view, three proteins directly

498 involved in calcium homeostasis/flux were identified (**Table 1** and **Table 2**), these being

499 ATP2A1: sarcoplasmic/endoplasmic reticulum calcium ATPase 1 and SRL: sarcalumenin from

500 the 110 kDa band and a voltage-dependent anion channel (VDAC3), an abundant protein of the

501 outer mitochondrial membrane from the 30 kDa band. Calcium ions have also been involved in

502 the apoptosis onset through some signalling pathways [1]. As mentioned above, apoptosis affects

503 the integrity of the skeletal muscle by the means of the modification of calcium flux during

504 aging and its consequences on protein proteolysis involving ultra-structural changes [49].

505 The sarcomeric α-actinins (ACTN2 and ACTN3) are the other structural proteins identified

506 in the 110 kDa band (**Table 1**). They are actin-binding proteins that operate as major structural

507 components of the contractile apparatus at the Z-disc to stabilize the cytoskeleton, playing a role

508 in signalling and metabolic functions[50]. According to an earlier study, ACTN2 is the major

509 component present in all skeletal muscle fibres compared to ACTN3 which has more specialized

510 expression pattern and is expressed only in fast glycolytic skeletal muscle fibres[50]. In this trial,

511 ACTN3 was identified also as a QTL of tenderness score confirming its importance (**Table 4**).

512 However, it is ACTN2 that is essential for the integrity of the contractile apparatus through a

513 multitude of interactions (**Figure 2g,h**). For example, it is able to anchor certain cytoskeletal and

514 sarcomeric proteins including nebulin[51] and also to link the vascular extracellular matrix

515 glycoproteins and fibrinogen complex to myofibrils (**Figure 3**). Therefore, any degradation of

516 actinins by endogenous proteases or calcium flux would affect the structure of the sarcomere,

517 especially the Z-disc region. Finally, the other actin-binding, and giant protein, we identified in

518 the 110 kDa band, is plectin (PLEC) which is also known as an intermediate filament-based

519 versatile cytolinker protein. This is the only one of the parent proteins which has not, to date,

been identified as a beef tenderness biomarker. However, it was very recently reported as being of importance in the p-m aging of pork[52]. Further studies are warranted on plectin biochemistry in beef muscle to reveal potential roles in beef aging process and tenderization.

110 kDa and 30 kDa bands are influenced by pathways related to energy metabolism, mitochondria, apoptosis, calcium homeostasis and fibrinogen complex

The presence of sarcoplasmic fragments and products from other organelles, especially those related to mitochondria were very evident from our proteomic analysis. In this study, fragments from metabolic proteins and associated pathways were the second most abundant p-m changes identified to migrate within the two protein bands of interest. It is conceivable that p-m events in the muscle can lead to the presence of sarcoplasmic fractions and products from other organelles. These findings are in keeping with the current body of knowledge around tenderness determination and the aging process of meat[1, 5, 13, 14]. For example, proteomic-based studies on p-m protein degradation using protein fragments extracted from beef muscle during aging showed that among the enzymes we identified, creatine kinase (CKM, discussed previously) and glycogen phosphorylase (PYGM) are degraded [30, 53] and both were calpain substrates [54]. It is worth noting that PYGM, a rate-limiting enzyme of glycogenolysis, was identified on chromosome 29 as a QTL for both sensory tenderness and shear force (**Table 4**). The identification of glycogen phosphorylase kinase β-subunit (PHKB), a regulatory enzyme of glycogen metabolism, in the 110 kDa band is consistent with the presence of PYGM. Calcium is the main regulator of PHKB[55] further supporting the identification of major proteins in the same band that play roles in calcium homeostasis (ATP2A1 and SRL presented above). Moreover, both PYGM and PHKB were related to pH decline (**Table 1**). OGDH (2-oxoglutarate dehydrogenase) and NNT (NAD(P) transhydrogenase) from the 110 kDa band and SLC25A11 (Mitochondrial 2-oxoglutarate/malate carrier protein) from the 30 kDa band are metabolic enzymes related to mitochondria (**Table 1** and **Table 2**). The three enzymes were previously

545 identified as biomarkers of beef tenderness[13], hence pointing their importance in beef aging.

546 OGDH catalyses the conversion of α- ketoglutarate to succinyl coenzyme A, a critical step in the

547 Krebs cycle, while SLC25A11 and NNT have multiple functions. NNT is involved in the

548 detoxification of reactive oxygen species and regulation of isocitrate dehydrogenase activity.

549 SLC25A11 catalyzes the transport of 2-oxoglutarate across the inner mitochondrial membrane

550 in an electroneutral exchange for malate or other dicarboxylic acids, and plays an important role

551 in several metabolic processes, including the malate-aspartate shuttle, the oxoglutarate/isocitrate

552 shuttle, and gluconeogenesis from lactate[56]. In addition, SLC25A11 maintains mitochondrial

553 fusion and fission events proposed to play a role in the conversion of muscle into meat[1], as well

554 as in the regulation of apoptosis. Other proteins from the 30 kDa fragment, these being PHB

555 (Prohibitin), CA3 (Carbonic anhydrase 3) and APOBEC2 (C->U-editing enzyme APOBEC-2)

556 were all identified as biomarkers of beef tenderness[13]. Among them, prohibitin plays several

557 roles especially in the morphogenesis of mitochondrial cristae including the mitochondrial

558 fusion and fission events[57]. CA3 is a marker of cell detoxification [1], known to be involved in the

559 regulation of the cellular pH in the living cell[58]. We suggest that CA3 would play a role in the

560 differences observed in the rates of pH decline among the four glycolysing groups of this trial.

561 Finally, we have revealed for the first time the presence in both bands of peptides related to

562 the fibrinogen complex with its three protein isoforms: FGA, FGB and FGG for fibrinogen α, β

563 and ɣ chains, respectively (**Table 1** and **Table 2**). Fibrinogen is known as extracellular matrix

564 (ECM) glycoproteins and categorized as vascular ECM proteins[59]. Fibrinogen, is a soluble

565 macromolecule, but forms a clot or insoluble gel on conversion to fibrin by the action of the

566 serine proteolytic enzyme thrombin[60]. We suppose that it is through prothrombin (F2) identified

567 in the 110 kDa fragment that fibrinogen was identified to be related to the tenderizing process of

568 meat. Also, fibrinogen has both strong and weak binding sites for calcium ions, which are

569 important for its structural stability and functions[60]. In its various functions as a clotting and

570 adhesive protein, the fibrinogen molecule is involved in many intermolecular interactions and

571   has specific binding sites for several proteins as shown in **Figure 2f** and **Figure 3**. In the context

572   of muscle to meat conversion, fibrinogen is not well studied. Thus, further investigations are

573   warranted to understand <mark>if it is a causative factor</mark> in p-m aging or if it is indicative of other

574   processes happening during this period *e.g.* aggregation, proteolysis etc.

575   To conclude, this study has revealed the first detailed map of several interconnected

576   pathways which are involved in the concomitant appearance of the 110 and 30 kDa SDS-PAGE

577   bands as two major proteolytic fragments among others appearing during aging/tenderizing

578   process of <mark>beef</mark> *Longissimus thoracis et lumborum* muscles. Interestingly, we have provided

579   strong evidence that the appearance of the fragments is pH decline dependent, being most

580   prevalent in fast glycolysing carcasses. This in-depth proteome analysis of the two protein bands

581   has revealed that most of the identified parent proteins have been identified as biomarkers of

582   beef tenderness and other quality traits, thus providing further clarity on the intricacies of these

583   relationships in light of p-m glycolytic rates. .

584   **Declaration of competing interest**

585   The authors declared that there is no conflict of interest.

586   **Acknowledgements**

596   Calvey and Mss. Shauna Morley from Dawn Meats Group; and Dr. Ruth Hamill, Dr. Carlos

597   Alvarez, Mr. Eugene Vesey and Mr. Yao Zhu from Teagasc, Ashtown.

598   **References**

599   1.   Ouali, A.; Gagaoua, M.; Boudida, Y.; Becila, S.; Boudjellal, A.; Herrera-Mendez, C. H.;
600   Sentandreu, M. A., Biomarkers of meat tenderness: present knowledge and perspectives in regards to our
601   current understanding of the mechanisms involved. *Meat science* **2013**, *95*, 854-70.

602   2.   Ouali, A., Meat Tenderization: Possible Causes and Mechanisms. A Review. *Journal of Muscle*
603   *Foods* **1990**, *1*, 129-165.

604   3.   Koohmaraie, M.; Geesink, G. H., Contribution of postmortem muscle biochemistry to the
605   delivery of consistent meat quality with particular focus on the calpain system. *Meat science* **2006**, *74*,
606   34-43.

607   4.   Gagaoua, M.; Hughes, J.; Terlouw, E. M. C.; Warner, R. D.; Purslow, P. P.; Lorenzo, J. M.;
608   Picard, B., Proteomic biomarkers of beef colour. *Trends in Food Science & Technology* **2020**, *101*, 234-
609   252.

610   5.   Picard, B.; Gagaoua, M., Meta-proteomics for the discovery of protein biomarkers of beef
611   tenderness: An overview of integrated studies. *Food Res Int* **2020**, *127*, 108739.

612   6.   Picard, B.; Gagaoua, M., Muscle Fiber Properties in Cattle and Their Relationships with Meat
613   Qualities: An Overview. *J Agric Food Chem* **2020**, *68*, 6021-6039.

614   7.   O'Halloran, G. R.; Troy, D. J.; Buckley, D. J.; Reville, W. J., The role of endogenous proteases
615   in the tenderisation of fast glycolysing muscle. *Meat science* **1997**, *47*, 187-210.

616   8.   Kemp, C. M.; Sensky, P. L.; Bardsley, R. G.; Buttery, P. J.; Parr, T., Tenderness--an enzymatic
617   view. *Meat science* **2010**, *84*, 248-56.

618   9.   Sentandreu, M. A.; Coulis, G.; Ouali, A., Role of muscle endopeptidases and their inhibitors in
619   meat tenderness. *Trends in Food Science & Technology* **2002**, *13*, 400-421.

620   10.   Gagaoua, M.; Hafid, K.; Boudida, Y.; Becila, S.; Ouali, A.; Picard, B.; Boudjellal, A.;
621   Sentandreu, M. A., Caspases and Thrombin Activity Regulation by Specific Serpin Inhibitors in Bovine
622   Skeletal Muscle. *Appl Biochem Biotechnol* **2015**, *177*, 279-303.

623   11.   Taylor, R. G.; Geesink, G. H.; Thompson, V. F.; Koohmaraie, M.; Goll, D. E., Is Z-disk
624   degradation responsible for postmortem tenderization? *Journal of Animal Science* **1995**, *73*, 1351-1367.

625   12.   Huff-Lonergan, E.; Zhang, W.; Lonergan, S. M., Biochemistry of postmortem muscle - lessons
626   on mechanisms of meat tenderization. *Meat science* **2010**, *86*, 184-95.

627   13.   Gagaoua, M.; Terlouw, E. M. C.; Mullen, A. M.; Franco, D.; Warner, R. D.; Lorenzo, J. M.;
628   Purslow, P. P.; Gerrard, D.; Hopkins, D. L.; Troy, D.; Picard, B., Molecular signatures of beef
629   tenderness: Underlying mechanisms based on integromics of protein biomarkers from multi-platform
630   proteomics studies. *Meat science* **2021**, *172*, 108311.

631   14.   Picard, B.; Gagaoua, M., Chapter 11 - Proteomic Investigations of Beef Tenderness. In
632   *Proteomics in Food Science: from farm to fork*, Colgrave, M. L., Ed. Academic Press: London, 2017; pp
633   177-197.

634   15.   Jia, X.; Hildrum, K. I.; Westad, F.; Kummen, E.; Aass, L.; Hollung, K., Changes in enzymes
635   associated with energy metabolism during the early post mortem period in longissimus thoracis bovine
636   muscle analyzed by proteomics. *J Proteome Res* **2006**, *5*, 1763-9.

637   16.   Laville, E.; Sayd, T.; Morzel, M.; Blinet, S.; Chambon, C.; Lepetit, J.; Renand, G.; Hocquette, J.
638   F., Proteome changes during meat aging in tough and tender beef suggest the importance of apoptosis
639   and protein solubility for beef aging and tenderization. *J Agric Food Chem* **2009**, *57*, 10755-64.

640   17.   White, A.; O'Sullivan, A.; Troy, D. J.; O'Neill, E. E., Manipulation of the pre-rigor glycolytic
641   behaviour of bovine M. longissimus dorsi in order to identify causes of inconsistencies in tenderness.
642   *Meat science* **2006**, *73*, 151-156.

643   18.   Lomiwes, D.; Farouk, M. M.; Wu, G.; Young, O. A., The development of meat tenderness is
644   likely to be compartmentalised by ultimate pH. *Meat science* **2014**, *96*, 646-651.

645   19.   Wu, G.; Farouk, M. M.; Clerens, S.; Rosenvold, K., Effect of beef ultimate pH and large
646   structural protein changes with aging on meat tenderness. *Meat science* **2014**, *98*, 637-45.

647   20.   Gagaoua, M.; Picard, B.; Monteils, V., Associations among animal, carcass, muscle
648   characteristics, and fresh meat color traits in Charolais cattle. *Meat science* **2018**, *140*, 145-156.

649   21.   Ponnampalam, E. N.; Hopkins, D. L.; Bruce, H.; Li, D.; Baldi, G.; Bekhit, A. E.-d., Causes and
650   Contributing Factors to "Dark Cutting" Meat: Current Trends and Future Directions: A Review.
651   *Comprehensive Reviews in Food Science and Food Safety* **2017**, *16*, 400-430.

652   22.   Hwang, I. H.; Thompson, J. M., The interaction between pH and temperature decline early
653   postmortem on the calpain system and objective tenderness in electrically stimulated beef longissimus
654   dorsi muscle. *Meat science* **2001**, *58*, 167-174.

655   23.   Zamora, F.; Aubry, L.; Sayd, T.; Lepetit, J.; Lebert, A.; Sentandreu, M. A.; Ouali, A., Serine
656   peptidase inhibitors, the best predictor of beef ageing amongst a large set of quantitative variables. *Meat
657   science* **2005**, *71*, 730-42.

658   24.   Laemmli, U. K., Cleavage of structural proteins during the assembly of the head of
659   bacteriophage T4. *Nature* **1970**, *227*, 680-5.

660   25.   Picard, B.; Kammoun, M.; Gagaoua, M.; Barboiron, C.; Meunier, B.; Chambon, C.; Cassar-
661   Malek, I., Calcium Homeostasis and Muscle Energy Metabolism Are Modified in HspB1-Null Mice.
662   *Proteomes* **2016**, *4*, 17.

663   26.   Gagaoua, M.; Picard, B.; Monteils, V., Assessment of cattle inter-individual cluster variability:
664   the potential of continuum data from the farm-to-fork for ultimate beef tenderness management. *J Sci
665   Food Agric* **2019**, *99*, 4129-4141.

666   27.   Koohmaraie, M.; Kennick, W. H.; Elgasim, E. A.; Anglemier, A. F., Effects of Postmortem
667   Storage on Muscle Protein Degradation: Analysis by SDS-Polyacrylamide Gel Electrophoresis. *Journal
668   of Food Science* **1984**, *49*, 292-293.

669   28.   Olson, D. G.; Parrish, F. C., Relationship of Myofibril Fragmentation Index to Measures of
670   Beefsteak Tenderness. *Journal of Food Science* **1977**, *42*, 506-509.

671   29.   Young, O. A.; Graafhuis, A. E.; Davey, C. L., Post-mortem changes in cytoskeletal proteins of
672   muscle. *Meat science* **1980**, *5*, 41-55.

673   30.   Troy, D.; Patyaryas, T.; Tsitsilonis, R.; Yialouris, P.; Vazeou, V.; Healy, A.; Stoeva, S.; Voelter,
674   W. In *Sequence analysis of proteins extracted from bovine myofibrillar extracts during the ageing*

675   *period*, ANNUAL INTERNATIONAL CONGRESS OF MEAT SCIENCE AND TECHNOLOGY,
676   1997; 1997; pp 698-699.

677   31.   Macbride, M. A.; Parrish, F. C., The 30,000-Dalton Component of Tender Bovine Longissimus
678   Muscle. *Journal of Food Science* **1977**, *42*, 1627-1629.

679   32.   Kołczak, T.; Pospiech, E.; Palka, K.; Łącki, J., Changes of myofibrillar and centrifugal drip
680   proteins and shear force of psoas major and minor and semitendinosus muscles from calves, heifers and
681   cows during post-mortem ageing. *Meat science* **2003**, *64*, 69-75.

682   33.   Penny, I. F.; Ferguson-Pryce, R., Measurement of autolysis in beef muscle homogenates. *Meat
683   science* **1979**, *3*, 121-134.

684   34.   Ho, C. Y.; Stromer, M. H.; Robson, R. M., Identification of the 30 kDa polypeptide in post
685   mortem skeletal muscle as a degradation product of troponin-T. *Biochimie* **1994**, *76*, 369-375.

686   35.   Negishi, H.; Yamamoto, E.; Kuwata, T., The origin of the 30 kDa component appearing during
687   post-mortem ageing of bovine muscle. *Meat science* **1996**, *42*, 289-303.

688   36.   Lana, A.; Zolla, L., Proteolysis in meat tenderization from the point of view of each single
689   protein: A proteomic perspective. *Journal of Proteomics* **2016**, *147*, 85-97.

690   37.   Wu, G.; Clerens, S.; Farouk, M. M., LC MS/MS identification of large structural proteins from
691   bull muscle and their degradation products during post mortem storage. *Food Chem* **2014**, *150*, 137-44.

692   38.   Pomponio, L.; Ertbjerg, P.; Karlsson, A. H.; Costa, L. N.; Lametsch, R., Influence of early pH
693   decline on calpain activity in porcine muscle. *Meat science* **2010**, *85*, 110-114.

694   39.   Huang, F.; Huang, M.; Zhou, G.; Xu, X.; Xue, M., In Vitro Proteolysis of Myofibrillar Proteins
695   from Beef Skeletal Muscle by Caspase-3 and Caspase-6. *Journal of Agricultural and Food Chemistry*
696   **2011**, *59*, 9658-9663.

697   40.   Kemp, C. M.; Bardsley, R. G.; Parr, T., Changes in caspase activity during the postmortem
698   conditioning period and its relationship to shear force in porcine longissimus muscle. *J Anim Sci* **2006**,
699   *84*, 2841-6.

700   41.   Robert, N.; Briand, M.; Taylor, R.; Briand, Y., The effect of proteasome on myofibrillar
701   structures in bovine skeletal muscle. *Meat science* **1999**, *51*, 149-153.

702   42.   Dutaud, D.; Aubry, L.; Guignot, F.; Vignon, X.; Monin, G.; Ouali, A., Bovine muscle 20S
703   proteasome. II: Contribution of the 20S proteasome to meat tenderization as revealed by an
704   ultrastructural approach. *Meat science* **2006**, *74*, 337-344.

705   43.   Mikami, M.; Whiting, A. H.; Taylor, M. A. J.; Maciewicz, R. A.; Etherington, D. J., Degradation
706   of myofibrils from rabbit, chicken and beef by cathepsin l and lysosomal lysates. *Meat science* **1987**, *21*,
707   81-97.

708   44.   Lange, S.; Pinotsis, N.; Agarkova, I.; Ehler, E., The M-band: The underestimated part of the
709   sarcomere. *Biochimica et Biophysica Acta (BBA) - Molecular Cell Research* **2020**, *1867*, 118440.

710   45.   Hornemann, T.; Kempa, S.; Himmel, M.; Hayeß, K.; Fürst, D. O.; Wallimann, T., Muscle-type
711   Creatine Kinase Interacts with Central Domains of the M-band Proteins Myomesin and M-protein.
712   *Journal of Molecular Biology* **2003**, *332*, 877-887.

713   46.   Ackermann, M. A.; Kontrogianni-Konstantopoulos, A., Myosin Binding Protein-C: A Regulator
714   of Actomyosin Interaction in Striated Muscle. *Journal of Biomedicine and Biotechnology* **2011**, *2011*,
715   636403.

716　47.　Fritz, J. D.; Greaser, M. L., Changes in Titin and Nebulin in Postmortem Bovine Muscle
717　Revealed by Gel Electrophoresis, Western Blotting and Immunofluorescence Microscopy. *Journal of*
718　*Food Science* **1991**, *56*, 607-610.

719　48.　Taylor, M. A. J.; Etherington, D. J., The solubilization of myofibrillar proteins by calcium ions.
720　*Meat science* **1991**, *29*, 211-219.

721　49.　Pinton, P.; Giorgi, C.; Siviero, R.; Zecchini, E.; Rizzuto, R., Calcium and apoptosis: ER-
722　mitochondria Ca2+ transfer in the control of apoptosis. *Oncogene* **2008**, *27*, 6407-6418.

723　50.　Lek, M.; Quinlan, K. G. R.; North, K. N., The evolution of skeletal muscle performance: gene
724　duplication and divergence of human sarcomeric α-actinins. *BioEssays* **2010**, *32*, 17-25.

725　51.　Nave, R.; Fürst, D. O.; Weber, K., Interaction of α-actinin and nebulin in vitro. *FEBS Letters*
726　**1990**, *269*, 163-166.

727　52.　Tian, X.; Wang, Y.; Fan, X.; Shi, Y.; Zhang, W.; Hou, Q.; Liu, R.; Zhou, G., Expression of Pork
728　Plectin during Postmortem Aging. *Journal of Agricultural and Food Chemistry* **2019**, *67*, 11718-11727.

729　53.　Stoeva, S.; Byrne, C. E.; Mullen, A. M.; Troy, D. J.; Voelter, W., Isolation and identification of
730　proteolytic fragments from TCA soluble extracts of bovine M. longissimus dorsi. *Food Chemistry* **2000**,
731　*69*, 365-370.

732　54.　Purintrapiban, J.; Wang, M.-c.; Forsberg, N. E., Identification of glycogen phosphorylase and
733　creatine kinase as calpain substrates in skeletal muscle. *The International Journal of Biochemistry & Cell*
734　*Biology* **2001**, *33*, 531-540.

735　55.　Brostrom, C. O.; Hunkeler, F. L.; Krebs, E. G., The regulation of skeletal muscle phosphorylase
736　kinase by Ca2+. *The Journal of biological chemistry* **1971**, *246*, 1961-7.

737　56.　Pan, G.; Wang, R.; Jia, S.; Li, Y.; Jiao, Y.; Liu, N., SLC25A11 serves as a novel prognostic
738　biomarker in liver cancer. *Scientific Reports* **2020**, *10*, 9871.

739　57.　Merkwirth, C.; Langer, T., Prohibitin function within mitochondria: Essential roles for cell
740　proliferation and cristae morphogenesis. *Biochimica et Biophysica Acta (BBA) - Molecular Cell*
741　*Research* **2009**, *1793*, 27-32.

742　58.　Duda, D. M.; Tu, C.; Fisher, S. Z.; An, H.; Yoshioka, C.; Govindasamy, L.; Laipis, P. J.;
743　Agbandje-McKenna, M.; Silverman, D. N.; McKenna, R., Human Carbonic Anhydrase III: Structural
744　and Kinetic Study of Catalysis and Proton Transfer. *Biochemistry* **2005**, *44*, 10046-10053.

745　59.　Hynes, R. O.; Naba, A., Overview of the Matrisome—An Inventory of Extracellular Matrix
746　Constituents and Functions. *Cold Spring Harbor Perspectives in Biology* **2012**, *4*.

747　60.　Weisel, J. W., Fibrinogen and Fibrin. In *Advances in Protein Chemistry*, Academic Press: 2005;
748　Vol. 70, pp 247-299.

749

750   **Figure captions**

751   **Figure 1.** pH decline and protein changes over p-m aging time. **a)** Scores plot of the separation of

752   the individuals (n = 6 per group) characterizing the four pH decline categories (with different

753   glycolysing rate): fast (F, ●), medium (M, ♦), slow (S, ▲) and very slow (VS, ■) using principal

754   component analysis. The loadings were based on pH values measured on carcass (10°C chill) at

755   the 4th lumbar from 1hr to 8hr p-m. **b)** Variance analysis comparing the calculated pH decline rates

756   (*k*) for each category at a significant level of 5%. **c)** Representative 1D SDS–PAGE profile of

757   Colloid Coomassie-stained (EZBlue® gel staining reagent) 12% polyacrylamide gel of beef *M.*

758   *longissimus thoracis et lumborum* muscle extracts at four different aging times starting from day 0

759   (biopsy samples taken at 3hr p-m). The first lane corresponds to the molecular weights (Mw)

760   standards in kiloDaltons (kDa). **d, e)** Densitometry analyses of the 110 and 30 kDa protein band

761   fragments appearing during p-m aging time as a function of pH decline (glycolysing rate) and

762   aging time (**Table S1** and **Table S2** for details of the variance analyses). The quantity changes of

763   the proteins were expressed in arbitrary units (means ± standard deviation). **f, g)** Exponential

764   curves representing formation of the 110 kDa and 30 kDa protein fragments over aging time. The

765   average estimate slopes of the curves are given for each pH decline category. **h)** Linear regression

766   between the protein quantities at day 14 p-m (D14) of the 110 kDa and 30 kDa protein fragments.

767   **Figure 2.** Biological pathways and process enrichment cluster analysis using Metascape®

768   (https://metascape.org/) on the 31 proteins identified from the two proteolytic 110 kDa and 30 kDa

769   band fragments. **a)** Circos plot showing the common 4 proteins between the 110 kDa and 30 kDa

770   proteolytic fragments. **b–d)** GO and KEGG analyses of the **b)** 22 proteins from the 110 kDa

771   fragment, **c)** 13 proteins from the 30 kDa fragment, and **d)** total 31 proteins from both fragments.

772   The bar graphs highlight the top enriched terms (functional clusters) across the protein lists

773   coloured according to *P*-values: terms with a *P*-value < 0.01, a minimum count of 3, and an

774   enrichment factor > 1.5. **e)** Heatmap based on the protein lists between the two proteolytic

775   fragments showing the top 8 enriched term clusters, one row per cluster, using a discrete colour

776   scale by *P*-values to represent statistical significance. Grey indicates a lack of significance. **f)**

777   Enrichment network visualization for results from the proteins present in each of the 8 clusters

778   identified coloured by cluster ID (details in **Table 3**), where nodes that share the same cluster ID

779   are typically close to each other. In the term networks, nodes are coloured by term, where terms

780   with a similarity >0.3 are connected by edges. **g)** Key most significant molecular complex

781   detection (MCODE) components form the network. Each node represents a protein, and the edge

782   between nodes represents the interaction between two connected proteins. **h)** The same MCODE

783   components (modules) by highlighting to which proteolytic fragment the proteins belong.

784   Abbreviations: GO *gene ontology*, KEGG *Kyoto Encyclopedia of Genes and Genomes pathways*.

785   **Figure 3.** Protein-protein interaction (PPI) network linking the whole 31 proteins from the 110 and

786   30 kDa proteolytic protein band fragments, highlighting also the molecular function. The

787   interaction map was generated from the web-based search STRING database (https://string-

788   db.org/). Network statistics are: number of nodes: 31; number of edges: 114; average node degree:

789   7.35; average local clustering coefficient: 0.735; expected number of edges: 9 and PPI enrichment

790   *p*-value: $< 1.0e^{-16}$. The secreted proteins among the 31 proteins were further shown by small

791   yellow ovals on each protein for those secreted using a signal peptide (conventional pathway) and

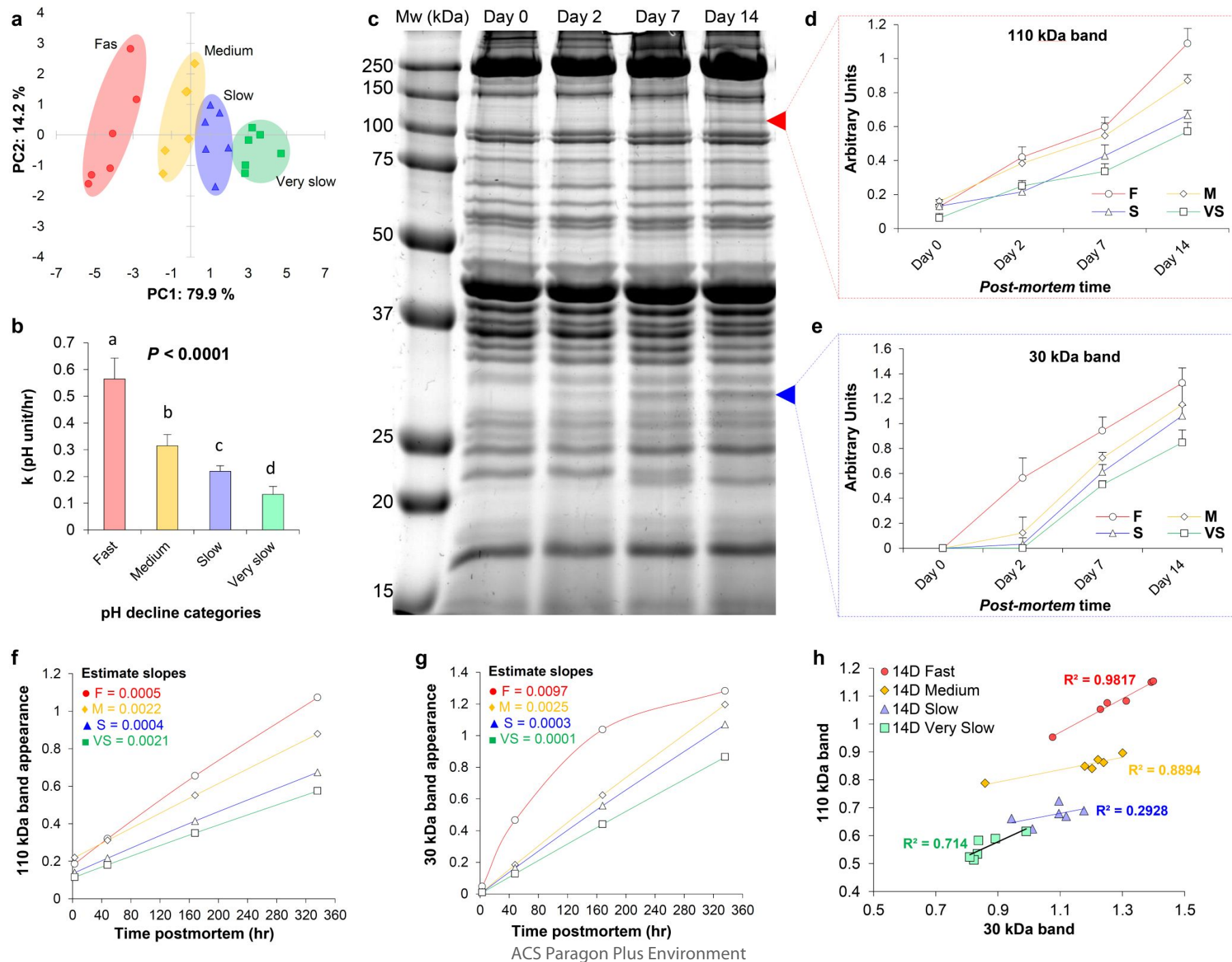792   by orange ovals for those pathways that do not involve a signal peptide.
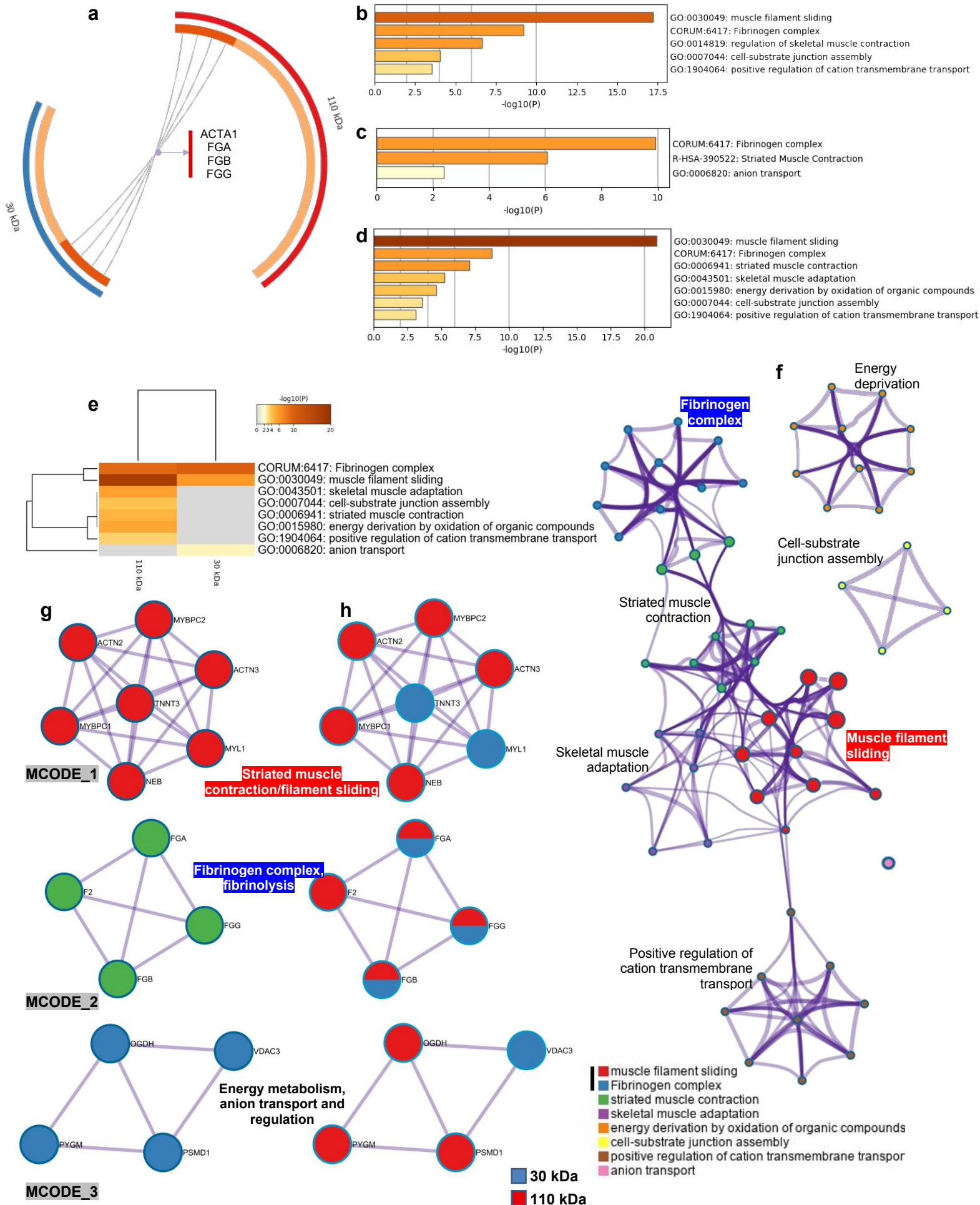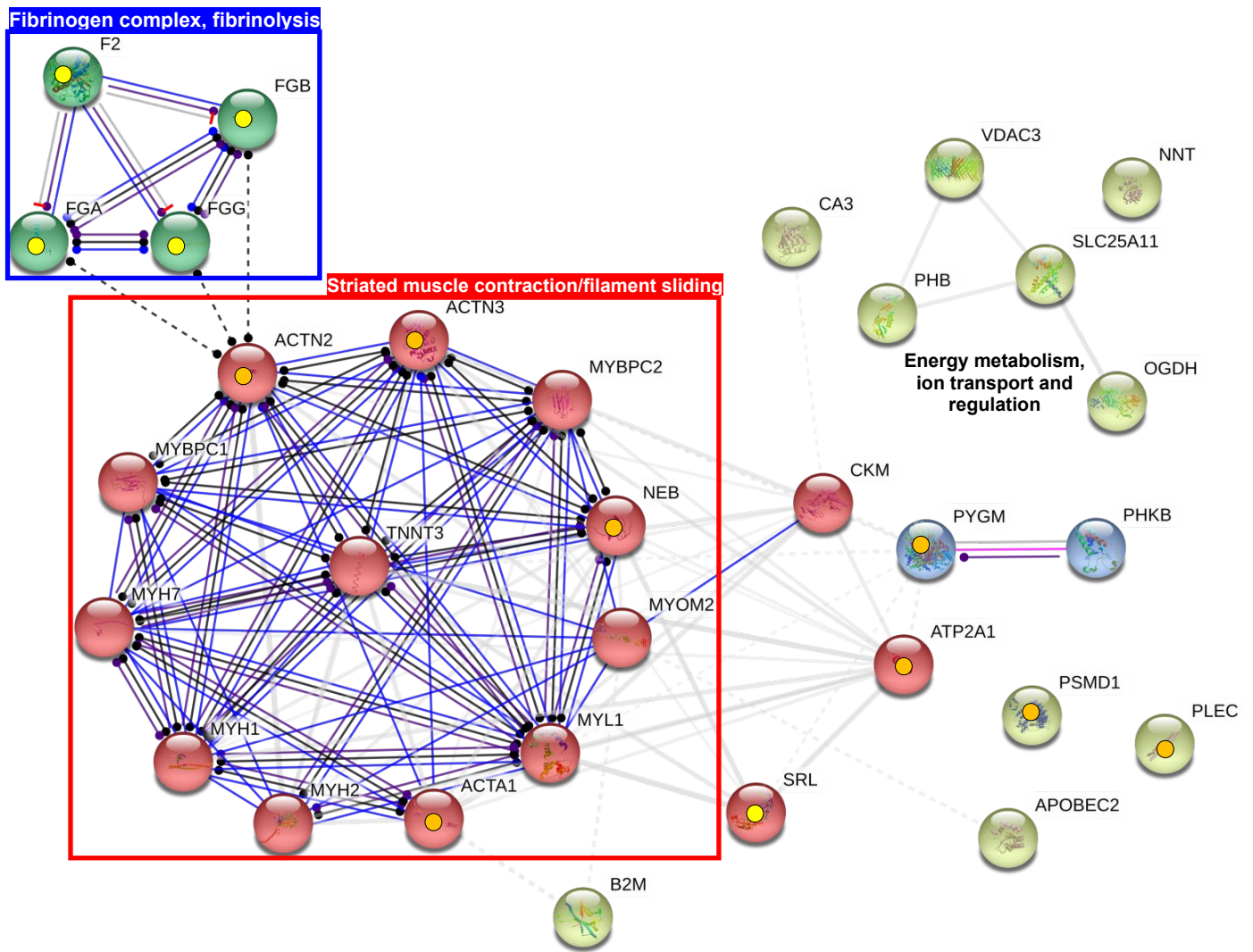
Figure 1.

Figure 2.

Figure 3.

Table 1. LC–MS/MS (Q Exactive HF-X) identified 22 proteins from the 110 kDa proteolytic fragment band separated by 12% 1D SDS–PAGE from beef *M. longissimus thoracis et lumborum* muscle during aging.

Accession number	Gene name	Full protein name	#Peptides	Coverage, %	Secreted protein [1]	Already identified in the literature (proteomics) to be related with beef		
						Tenderness [2]	Colour [3]	pH drop
Muscle contraction and structure								
Q9BE39	MYH7	Myosin-7	21	34.26	✘	✔	✔	✔
Q9BE41	MYH2	Myosin-2	44	40.98	✘	✔	✔	✔
Q9BE40	MYH1	Myosin-1	52	45.15	✘	✔	✔	✔
P68138	ACTA1	Actin, alpha skeletal muscle	13	44.30	✔✔	✔	✔	✔
Q3ZC55	ACTN2	Alpha-actinin-2	22	28.30	✔✔	✔	✘	✔
Q0III9	ACTN3	Alpha-actinin-3	30	40.84	✔✔	✔	✔	✘
A0A3Q1MC60	NEB	Nebulin	22	4.84	✔✔	✔	✘	✘, sheep
E1BF59	PLEC	Plectin	30	8.24	✔✔	✘, pork	✘	✘, pork
A6QP89	MYBPC1	Myosin-binding protein C, slow-type	36	39.23	✘	✔	✔	✘
E1BNV1	MYBPC2	Myosin-binding protein C, fast-type	12	37.77	✘	✔	✘, isoform yes	✘
E1BF23	MYOM2	Myomesin-2	17	30.70	✘	✔	✔	✔
Catalytic and energy metabolism								
P79334	PYGM	Glycogen phosphorylase, muscle form	10	26.48	✔✔	✔	✔	✔
Q148N0	OGDH	2-oxoglutarate dehydrogenase, mitochondrial	5	4.59	✘	✔	✘	✘
F1MJ90	PHKB	Glycogen phosphorylase kinase β-subunit	12	21.86	✘	✘	✘	✔
P11024	NNT	NAD(P) transhydrogenase, mitochondrial	6	7.92	✘	✔	✘	✔
Vascular ECM glycoproteins and fibrinogen complex								
P02672	FGA	Fibrinogen alpha chain	12	32.03	✔	✘, pork	✘, isoform yes	✘
P02676	FGB	Fibrinogen beta chain	11	44.65	✔	✘, pork	✔	✘
P12799	FGG	Fibrinogen gamma chain	6	33.33	✔	✘, pork	✘, isoform yes	✘
Proteolysis								
P00735	F2	Prothrombin	4	5.28	✔	✔	✘	✘
A7MBA2	PSMD1	26S proteasome non-ATPase regulatory subunit 1	4	3.99	✔✔	✔	✘, isoform yes	✘
Calcium binding and apoptotic mitochondrial changes								
Q0VCY0	ATP2A1	Sarcoplasmic/endoplasmic reticulum calcium ATPase 1	12	15.21	✔✔	✔	✘, isoform yes	✔
F1MJW7	SRL	Sarcalumenin	9	17.19	✔	✔	✘	✘, pork

[1] Prediction of secreted proteins was performed by the ProteINSIDE tool (http://www.proteinside.org/) identifying those potentially secreted through a signal peptide (✔) using the Signal P algorithm and by pathways that do not involve a signal peptide (✔✔) using the TargetP algorithm. If not validated, this was mentioned by a "✘".

[2] The validation (✔) was mostly performed based on the integromics database on beef tenderness biomarkers from Gagaoua *et al.*[13] and also from other studies, species and muscles if not found in the corpus. If the protein isoform instead of the protein in question that is identified, this was accordingly specified.

[3] The validation was mostly performed based on the integromics database on beef colour biomarkers from Gagaoua *et al.*[4] and also from other studies, species and muscles if not found in the corpus.

Table 2. LC–MS/MS (Q Exactive HF-X) identified 13 proteins from the 30 kDa proteolytic fragment band separated by 12% 1D SDS–PAGE from <mark>beef</mark> *M. longissimus thoracis et lumborum* muscle during aging.

Accession number	Gene name	Full protein name	#Peptides	Coverage, %	Secreted protein[1]	Already identified in the literature (proteomics) to be related with beef		
						Tenderness[2]	Colour[3]	pH drop
Muscle contraction and structure								
P68138	ACTA1[4]	Actin, alpha skeletal muscle	13	44.30	✓✓	✓	✓	✓
Q8MKI3	TNNT3	Troponin T, fast skeletal muscle	20	42.07	✗	✓	✗	✗, pork
A0JNJ5	MYL1	Myosin light chain 1/3, skeletal muscle isoform	17	73.96	✗	✓	✓	✓
Catalytic and energy metabolism								
Q9XSC6	CKM	Creatine kinase M-type	8	46.19	✗	✓	✓	✓
P22292	SLC25A11	Mitochondrial 2-oxoglutarate/malate carrier protein	4	19.75	✗	✓	✗	✗
Vascular ECM glycoproteins and fibrinogen complex								
P02672	FGA[4]	Fibrinogen alpha chain	12	32.03	✓	✗, pork	✗, isoform yes	✗
P02676	FGB[4]	Fibrinogen beta chain	11	44.65	✓	✗, pork	✓	✗
P12799	FGG[4]	Fibrinogen gamma chain	6	33.33	✓	✗, pork	✗, isoform yes	✗
Protein-binding, calcium, ion transport and apoptosis								
P01888	B2M	Beta-2-microglobulin	6	42.07	✓	✗, pork	✗	✗, pork
Q9MZ13	VDAC3	Voltage-dependent anion-selective channel protein 3	4	19.64	✓✓	✓	✗	✓
Q3T165	PHB	Prohibitin	4	18.75	✓✓	✓	✗	✗, pork
Q3SZX4	CA3	Carbonic anhydrase 3	4	17.69	✗	✓	✓	✓
Q3SYR3	APOBEC2	C->U-editing enzyme APOBEC-2	5	21.88	✗	✓	✓	✗

[1] Prediction of secreted proteins was performed by the ProteINSIDE tool (http://www.proteinside.org/) identifying those potentially secreted through a signal peptide (✓) using the Signal P algorithm and by pathways that do not involve a signal peptide (✓✓) using the TargetP algorithm. If not validated, this was mentioned by a "✗".

[2] The validation (✓) was mostly performed based on the integromics database on beef tenderness biomarkers from Gagaoua *et al.*[13] and also from other studies, species and muscles if not found in the corpus. If the protein isoform instead of the protein in question that is identified, this was accordingly specified.

[3] The validation was mostly performed based on the integromics database on beef colour biomarkers from Gagaoua *et al.*[4] and also from other studies, species and muscles if not found in the corpus.

[4] Common proteins with the 110 kDa protein fragment band.

Table 3. Top 8 significant clusters with their representative enriched terms (one per cluster) using the total 31 proteins identified from the two proteolytic bands (110 and 30 kDa).

Pattern [1]	Gene Ontology	Category	Description	Count [2]	% [3]	Log10(P) [4]	Log10(q) [5]
■■	GO:0030049	GO Biological Processes	muscle filament sliding	10	32.26	-20.87	-16.86
■■	CORUM:6417	CORUM	Fibrinogen complex	3	23.08	-9.93	-6.53
■	GO:0006941	GO Biological Processes	striated muscle contraction	6	19.35	-7.08	-3.96
■	GO:0043501	GO Biological Processes	skeletal muscle adaptation	3	13.64	-5.69	-3.2
■	GO:0015980	GO Biological Processes	energy derivation by oxidation of organic compounds	5	22.73	-5.37	-2.99
■	GO:0007044	GO Biological Processes	cell-substrate junction assembly	3	13.64	-4.02	-2.01
■	GO:1904064	GO Biological Processes	positive regulation of cation transmembrane transport	3	13.64	-3.54	-1.61
■	GO:0006820	GO Biological Processes	anion transport	3	23.08	-2.38	-0.64

[1] The colour code used to distinguish the protein lists among the two proteolytic bands, ■ 110 kDa and ■ 30 kDa, where the term is found statistically significant, *i.e.,* multiple colours indicate a pathway/process that is shared across the two protein lists.

[2] The number of protein names from the 33 proteins related to proteolysis of the fragments 110 and 30 kDa with membership in the given ontology term.

[3] Percentage of protein among the total list of proteins found in the given ontology term (only input genes with at least one ontology term annotation are included in the calculation).
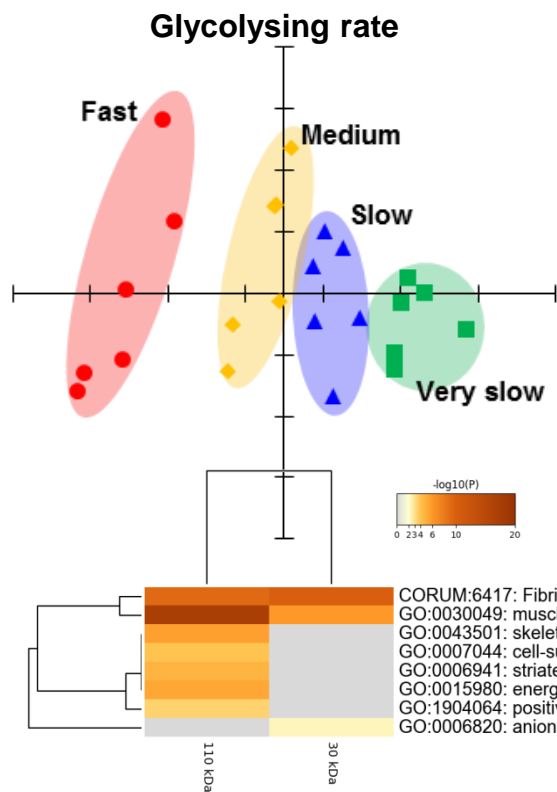
[4] The *p*-value in log base 10.

[5] The multi-test adjusted *p*-value in log base 10. An adjusted (Benjamini–Hochberg corrected) *p*-value < 0.05 was considered as the threshold for statistical significance.
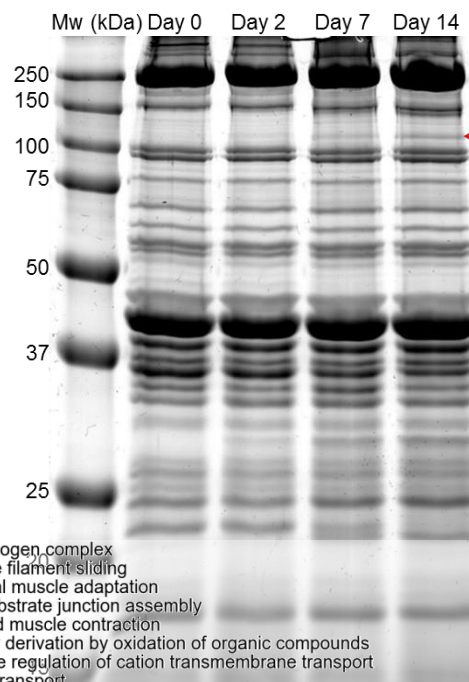
Table 4. Quantitative trait loci (QTL) of meat quality traits among the list of 31 identified proteins in the 110 and 30 kDa protein bands (fragments) from beef

M. longissimus thoracis et lumborum related to beef tenderness (sensory and shear force) and meat colour lightness (*L**).

QTL linked to QTLdb [a]	Gene Name	Proteolytic band (fragment)	Full protein Name	UniProt ID	Chromosome
Tenderness score	TNNT3	30 kDa	Troponin T, fast skeletal muscle	Q8MKI4	Chr.29
	ACTN3	110 kDa	Alpha-actinin-3	Q0III9	Chr.29
	PYGM	110 kDa	Glycogen phosphorylase, muscle form	P79334	Chr.29
Shear force	PYGM	110 kDa	Glycogen phosphorylase, muscle form	P79334	Chr.29
	MYBPC1	110 kDa	Myosin binding protein C, slow type	E1BNV1	Chr.5
	F2	110 kDa	Prothrombin	P00735	Chr.15
	CA3	30 kDa	Carbonic anhydrase 3	Q3SZX4	Chr.14
	VDAC3	30 kDa	Voltage-dependent anion-selective channel protein 3	Q9MZ13	Chr.27
Meat color *L**	CKM	30 kDa	Creatine kinase M-type	Q9XSC6	Chr.18
	PHB	30 kDa	Prohibitin	Q3T165	Chr.19

[a] ProteQTL tool included in ProteINSIDE tool (http://www.proteinside.org/) interrogates a public library of published QTL in the Animal QTL Database (https://www.animalgenome.org/QTLdb/) that contains cattle QTL and association data curated from published scientific articles.

Glycolysing rate

Post-mortem aging of beef

New proteolytic fragments